

DEVELOPMENT OF LOW-ENERGY HEAVY-ION BEAMS BY THE RIKEN AVF CYCLOTRON AND HYPER ECR ION SOURCE OF CNS

Y. Kotaka[#], Y. Ohshiro, S. Watanabe, H. Yamaguchi, N. Imai,
S. Shimoura, Center for Nuclear Study, University of Tokyo, Wako, Saitama, Japan
M. Kase, S. Kubono, Riken Nishina Center, RIKEN, Wako, Saitama, Japan
K. Hatanaka, Research Center for Nuclear Physics, Osaka University, Ibaraki, Osaka, Japan
A. Goto, Yamagata University, Yamagata, Yamagata, Japan
H. Muto, Center of General Education, Tokyo University of Science, Chino, Nagano, Japan

Abstract

The first of three categories of the upgrade of RIKEN AVF cyclotron is to expand a variety of metal ion beams using Hyper ECR ion source. The non-axial rod method, multi-hole micro-oven method and plasma spectroscopy was developed. The second is to increase acceleration energy. By the beam simulation, the center region was renovated and ${}^4\text{He}^{2+}$ 12.5 MeV/u ion beam can be available. The third is to increase beam intensity. For injection, a pepper-pot emittance monitor is developed for the purpose of measuring a four-dimensional phase space distribution. For extraction, flat top system was developed. Using a faraday cup installed at the exit of deflector, the extraction efficiency is improved. For the transmission efficiency from AVF cyclotron to CNS RI Beam separator, the redesign of beam transport system is planned.

INTRODUCTION

RIKEN AVF cyclotron was built in 1989. This original design is the following. RF frequency range is 12-24 MHz. The acceleration harmonics is 2. Maximal RF voltage is 50 kV. Average magnetic field range at the extraction is 0.5-1.76 T. K-value is 70.

The upgrade of AVF cyclotron has been conducted since 2000 by a collaboration of the Center for Nuclear Study (CNS) of the University of Tokyo and RIKEN Nishina Center to meet the request of CNS RI Beam separator (CRIB) which can produce the low energy RI beam to study nuclear astrophysics [1].



Figure 1: The schematic view of Hyper ECRIS, AVF cyclotron and CRIB with beam transport line.

We have three categories of the upgrades. One is to expand a variety of ion species. Two is to expand the region of available acceleration energy. Three is to increase beam intensity. Each will be in the following.

Besides, nondestructive beam monitors, Scanner [2] and Core Monitor [3], were developed to see stability.

Figure 1 shows the location of AVF cyclotron, Hyper ECR ion source (ECRIS), CRIB and the several diagnostics.

EXPAND ION SPECIES

We have developed two methods for feeding vapor of solid materials into the plasma by ECRIS in order to expand the ion species as well as increasing the beam intensity stably [4]. One is the non-axial rod method applied for CaO, SiO₂ and FeO, operating up to 2600 degrees. Since the tip of the material rod is placed near the wall of plasma chamber, the constant vapor rate of material is obtained. Two is the multi-hole micro-oven method applied for P₂O₅, Li, and S, operating up to 800 degrees. We can control the vapor rate with the number of holes of crucible. The beam intensities extracted from the ECRIS are listed in Table 1 together with melting point.

Table 1: Solid Ion Species Ionized by Hyper ECRIS

Ion Species	Beam Intensities (eμA)	Charged Material	m.p. (°C)
${}^6\text{Li}^{2+}$	200→280	Li pure metal (Oven)	180
${}^6\text{Li}^{3+}$	34→75	Li pure metal (Oven)	180
${}^{10}\text{B}^{4+}$	50	B ₁₀ H ₁₄ (¹⁰ B-99.9, MIVOC)	99
${}^{11}\text{B}^{4+}$	50	B ₁₀ H ₁₄ (MIVOC)	99
${}^{24}\text{Mg}^{8+}$	30→45	Mg pure metal (Oven)	650
${}^{28}\text{Si}^{8+}$	32→35	SiO ₂ (Rod)	1500
${}^{31}\text{P}^{8+}$	29	P ₂ O ₅ (Oven)	563
${}^{32}\text{S}^{9+}$	47	S grain (Oven)	119
${}^{40}\text{Ca}^{12+}$	25	CaO (Rod)	2572
${}^{56}\text{Fe}^{15+}$	7→15	FeO (Rod)	1420
${}^{58}\text{Ni}^{15+}$	13	C ₁₀ H ₁₀ Ni (MIVOC)	173
${}^{59}\text{Co}^{15+}$	7→20	Co pure metal (Rod)	1493
${}^{87}\text{Rb}^{20+}$	1.2	RbCl (Oven)	682

Plasma spectroscopy has been developed in order to separate the desired ion species from the same m/q ion species in the plasma. The method is to observe the light intensity of the desired ion species by a grating monochromator. We confirmed the relation between the light intensity of an optical line spectrum of ${}^6\text{Li}^{3+}$ and its beam intensity measured by the faraday cup (FC) located at the exit of AVF cyclotron. Therefore, we can apply the light intensity to the beam intensity [5]. By this method, the tuning efficiency of ECRIS has been improved.

EXPAND ENERGY REGION

For the request of $^{15}\text{N}^{5+}$ 9 MeV/u ion beam, K-value and RF voltage needs 81 and 56 kV, respectively. At first, we improved the maximum output current of main and some trim coils power supply so that K-value was increased to 78 and $^{15}\text{N}^{5+}$ 8.67 MeV/u ion beam was available [6]. However, this has not been realized yet because the cooling capacity of main coil is not enough and the wideband amplifier of RF is unimproved.

$^{16}\text{O}^{7+}$ and $^6\text{Li}^{3+}$ 12 MeV/u ion beams were also requested with the high intensity beam. Due to the original design of AVF cyclotron, the maximal energy of $^6\text{Li}^{3+}$ and $^{16}\text{O}^{7+}$ ion beams had been respectively up to 9.7 MeV/u and 9.0 MeV/u at that time.

To meet the request, we focused on the beam dynamics simulation using the computed 3D electromagnetic fields [7] [8] [9]. The result indicated that it was possible to expand the region of available acceleration energy as well as improving injection efficiency by modifying the central region geometry [10] [11].

The renovation of the center region was carried out in august 2009. The energy of $^{16}\text{O}^{7+}$ and $^6\text{Li}^{3+}$ has been up to 11.2 MeV/u by now. Moreover, we succeeded $^4\text{He}^{2+}$ 12.5 MeV/u ion beam, whose intensity is 10.7 μA , is available. This injection efficiency is successfully 0.26, which is close to the average injection efficiency 0.31.

INCREASE BEAM INTENSITY

Improve Injection Efficiency

Injection efficiency goes down as the ECRIS beam intensity increases and scatters widely (Fig.2). In order to improve this, we began to study the beam emittance.

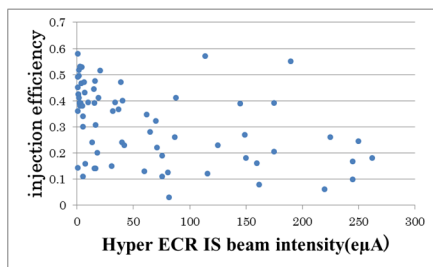


Figure 2: The relationship between injection efficiency and ECRIS beam intensity.

Since some solenoid coils exist in injection beam line, horizontal (x) and vertical (y) beam elements can be coupled. Considering it was important, we focused a four-dimensional phase space (x, x', y, y'). At first, we studied the beam simulation of ECRIS. Then, we started a pepper-pot emittance measurement [12].

The measurement principle is indicated in the left of Fig.3. A pepper-pot which is a plate with holes arranged in a square lattice shape is set perpendicular to beam axis. The beam passing through the holes reaches Detector set at the back. Each beam-spot measured by Detector can have a certain corresponding hole of pepper-pot like (x1, y1) and

(x2, y2). Using the distance (L) between pepper-pot and Detector, the angle can be calculated.

We have developed a pepper-pot emittance monitor (the right of Fig.3). The diameter of hole is 0.3 mm. Each distance of adjacent hole is 3 mm.

Since we selected the viewer plate coated by KBr phosphor as Detector, the beam image can be recorded by digital camera. We assume the beam intensity would be proportional to pixel size of digital image. Viewer plate is inclined at 45 degrees against beam axis because the beam image is seen through the view port. L is 55 mm.

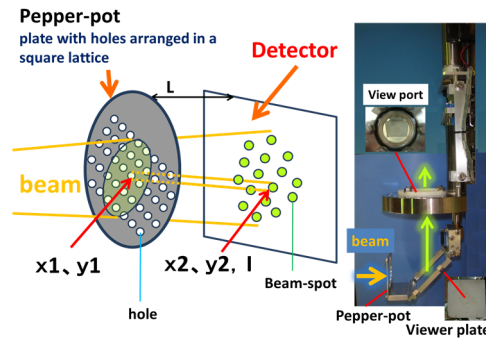


Figure 3: The schematic view of pepper-pot emittance measurement (left) and developed monitor (right).

To see the performance, we irradiated this monitor, installed at Pepperpot_IH10 (Fig.1), with $^4\text{He}^{2+}$ 20 keV ion beam of 51 μA from ECRIS. The red frame of Fig.4 indicates the recorded image. Using this image and the positions of pepper-pot holes, we calculated the four-dimensional phase space distribution.

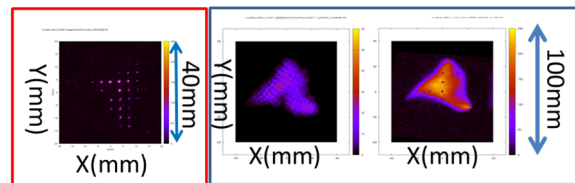


Figure 4: The beam image of pepperpot_IH10 (red frame). The image transported to the point of I23viewer from pepperpot_IH10 (the left of blue frame) and the beam image of I23viewer (the right of blue frame).

In order to see the performance, we transported this distribution to the two points of the beam line where I23viewer and EM_I36 are indicated in the Fig.1.

At first, we show the (x, y) distribution transported to I23viewer in the left of blue frame of Fig.4 and the beam image of I23viewer in the right. The transported (x, y) distribution is close to the I23viewer beam image.

Second, Fig.5 indicates the following. The left column shows the calculated emittances of the distribution transported to the point of EM_I36. The right column shows the measured emittances by the slit type emittance monitor installed at EM_I36. The (u, w) coordinate system is rotated 45 degrees with respect to (x, y).

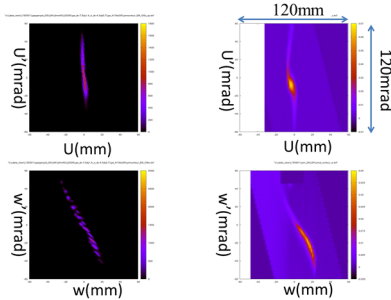


Figure 5: Left and right column show respectively the calculated emittances and measured emittances of EM_I36. Upper row is (u, u') and lower row is (w, w').

The calculated emittances have some disappeared parts compared with the measured emittance. We guess the reason why the sensitivity is zero for low intensity beam. Allowing for the guess, the calculated emittance is close to the measured emittance.

Improve Extraction Efficiency

Extraction efficiency is defined as beam transmission ratio through the deflector, magnetic-channel (MC) and gradient-collector (GC). In order to improve extraction efficiency, we developed flat top system (FT) [13].

FT was found to be effective. However, the discharge frequently occurred in the RF amplifier due to FT. We attempted to constrain the discharge so that the main and FT voltage were stably able to generate at 45 kV and 5 kV respectively when RF frequency was 16.3 MHz [14]. At the moment, we refrained from using FT in order to provide the stable beam to user.

In order to measure the beam intensity of the exit of deflector, we installed FC there in January 2010. Using it, we researched the beam loss and found that GC had to be corrected. As a result, the extraction efficiency after 2010 is improved compared with the one of 2006-2007 (Fig.6).

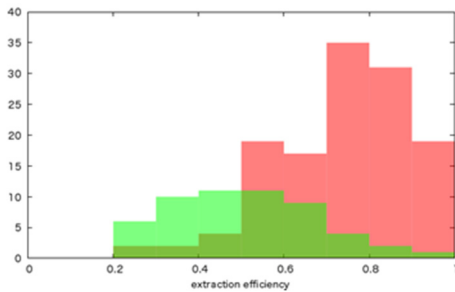


Figure 6: The distribution of extraction efficiency in 2010-2015(red box) and 2006-2007(green box).

Improve Transmission Efficiency to CRIB

The average transmission efficiency from AVF cyclotron to CRIB is 70 %. The loss must be recovered.

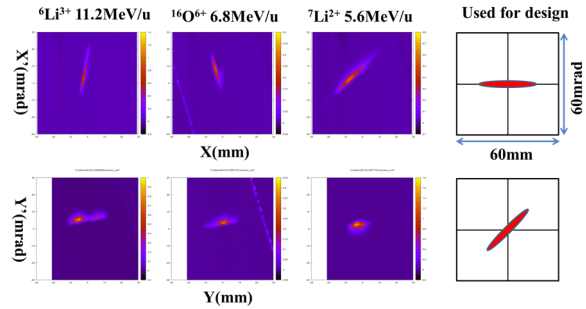


Figure 7: Columns from 1st to 3rd are the measured emittances. 4th column is the emittance used for design. Upper and lower rows indicate respectively a horizontal emittance and a vertical emittance.

We have measured the emittance by the slit type emittance monitor installed at EM_C01 (Fig.1) since 2012. We found the measured emittances differ from the emittance used for designing the beam transport system from AVF cyclotron to CRIB (Fig.7). Considering the difference is one reason for the low transmission efficiency, we will redesign the beam transport system.

SUMMARY AND CONCLUSION

We have supplied CRIB since 2000 with ion beams indicated in the Table 2, which also shows the beam time and RI beam produced by CRIB. Total beam time is 10283.2 hours. The average transmission efficiency from Hyper ECRIS to CRIB has been 0.065 since 2012. In order to improve this, we currently concentrate on the improvement of injection efficiency and transmission efficiency from AVF cyclotron to CRIB.

Table 2: Ion Beams and Beam Times Supplied to CRIB

ion species	energy(MeV/u)	beam time(hr)	RI beam produced by CRIB
⁶ Li ³⁺	9.5, 11.2	482.2	⁸ B
⁷ Li ^{3+,2+}	3.4, 3.5, 5.0, 5.5, 5.6, 8.6, 8.8	1230.4	⁷ Be, ⁸ Li
¹⁰ B ⁴⁺	7.8, 8.5	497.1	¹⁰ C, ¹¹ C, ¹² N
¹¹ B ³⁺	4.6, 5.0	521.5	¹⁰ Be, ¹¹ C
¹³ C ⁴⁺	6	124.8	¹³ N
¹⁴ N ^{6+,5+}	6.4, 7.0, 8.2, 8.4	1112.9	¹¹ C, ¹⁴ O, commissioning, test
¹⁵ N ^{5+,4+}	5.0, 5.5, 7.0	552.3	¹⁵ O, ¹⁶ N
¹⁶ O ^{7+,6+}	6.3, 6.8, 10.3, 11	810.2	¹⁷ F, ¹⁷ Ne, ¹⁸ Ne
¹⁸ O ⁶⁺	3.9, 4.0, 4.5, 5.9, 6.1, 7.0	1214.6	¹⁴ C, ¹⁷ N, ¹⁷ O, ¹⁸ N, ¹⁸ O, ¹⁸ F, ¹⁸ Ne
²⁰ Ne ^{8+,7+,6+}	6.0, 6.2, 6.3, 6.5, 8.2	1118.7	²¹ Na, ²² Mg
²² Ne ⁷⁺	6.1	364.7	²² NaI
²⁴ Mg ⁸⁺	7.5	975.2	²³ Mg, ²⁵ Al, ²⁶ S
²⁸ Si ^{10+,9+}	4.8, 6.9, 7.4, 7.5	519.1	³⁰ P, ³⁰ S
³¹ P ⁹⁺	6	37.4	³⁰ P
³⁶ Ar ¹⁰⁺	3.6	379.1	⁴⁶ Ti, ⁴⁶ Cr
⁴⁰ Ar ¹¹⁺	4.5	174.8	³⁹ Ar, ⁴⁹ V
⁴⁰ Ca ¹²⁺	5.5, 5.6	67.1	⁴⁰ Cr, ⁴⁹ Cr
⁴² Ca ¹²⁺	5.9	101.1	⁴⁴ Ti

REFERENCE

[1] Y.Yanagisawa et al., Nucl. Instr. and Meth. Phys. Res., **A539** (2005) 74
 [2] S.Watanabe et al., CNS Annual Report 2011 (2013) 82

- [3] S.Watanabe et al., Nucl. Instrum. and Meth. **A633** (2011) 8
- [4] Y.Oshiro et al., Rev. Sci. Instr. 85, 02A912 (2014)
- [5] H. Muto et al., Rev. Sci. Instr. 85 (2014) 02A905
- [6] S.Watanabe et al., CNS Annual Report 2005 (2006) 55
- [7] A.S.Vorozhtsov et al., RIKEN-NC-AC-2
- [8] E.E.Perepelkin et al., RuPAC 2008 (2008) p40
- [9] S.B. Vorozhtsov et al., RuPAC 2008 (2008) p51
- [10] S.B. Vorozhtsov et al., Proc. Particle Accelerator Society Meeting 2009 p240
- [11] A.Goto et al. RIKEN Accel. Prog. Rep. 43 (2010) 127
- [12] T.Hoffmann et al., Proc. 9th BIW 2000, Cambridge, USA, PP.432-439
- [13] S.Kohara et al., Nucl. Instrum. and Meth. **A526** (2004) 230
- [14] S.Kohara et al. RIKEN Accel. Prog. Rep. 39 2005(2006) 23